Journal of Applied Electrochemistry (2005) 35:529–537
DOI 10.1007/s10800-005-1318-3

Electrochemical behavior of coupled carbon fiber-reinforced polymer (CFRP) rods in concrete

A.A. TORRES-ACOSTA[1,*,†] and R. SEN[2]
[1]*Postgraduate and Research Coordinator, Universidad Marista de Queretaro, 2 Marte Avenue, 76000, Queretaro, Mexico*
[2]*Department of Civil and Environmental Engineering, University of South Florida, Room ENB-118, 4202 East Fowler Avenue, Tampa, FL, 33620, USA*
*(*author for correspondence, e-mail: atorres@imt.mx)*
[†]*Permanent address: Instituto Mexicano del Transporte, Sanfandila, Queretaro, Mexico*

Received 11 March 2004; accepted in revised form 20 December 2004

Key words: CFRP, concrete, EIS, epoxy coated rebar, galvanic corrosion, steel reinforcement

Abstract

This paper presents results on the electrochemical behavior of carbon fiber-reinforced polymer (CFRP) composite rods in contact with steel or epoxy coated steel bars in chloride-contaminated concrete. Twelve concrete prisms reinforced by CFRP rods electrically connected to plain or epoxy coated rebars were exposed to 80% humidity for 345 days. Four identical specimens that were not electrically connected served as controls. Measured galvanic currents densities were found to be as much as 100 μA cm^{-2}, raising concerns about the degradation of both CFRP and steel. Electrochemical impedance spectroscopy (EIS) tests were performed to detect possible changes in the electrochemical parameters of CFRP due to galvanic interaction with active steel. Equivalent circuit simulations of the pre- and post-galvanic interaction of CFRP rods with active steel were also evaluated. EIS data indicated that the composite surface was altered so as to have porous electrode characteristics. Optical microscopy provided visible evidence of interface changes on the composite surface, supporting EIS data. The preliminary findings suggest that it would be unwise to permit CFRP to be directly in contact with steel in reinforcing or prestressing applications.

1. Introduction

Carbon fiber reinforced polymers (CFRPs) have emerged as a new structural material in construction and increasingly for the repair and rehabilitation of both concrete [1] and steel structures [2]. In new construction, unidirectional CFRP is embedded inside concrete in reinforcing and prestressing applications usually in conjunction with epoxy-coated steel that can resist multi-directional web stresses. If the epoxy coating remains intact, no coupling between steel and CFRP occurs and therefore there is no possibility of galvanic action. However, experience in Florida and elsewhere suggests that some breaks in the epoxy coating during construction are inevitable. It has been estimated that breaks of the order of a fraction of 1% of the surface area are not unreasonable [3]. Where such breaks occur and the CFRP rod and steel are in direct contact, galvanic action takes place, since carbon develops a very noble potential in chloride-contaminated alkaline media (e.g. calcium hydroxide solution, mortar, concrete), as compared with steel [4–7].

A similar situation can occur in repair and rehabilitation of steel structures where chlorides from de-icing salts can create favorable conditions for galvanic action. Here the suggested remedy is the placement of a glass fiber barrier between the CFRP plate and the steel to prevent direct contact. However, given the differences in thermal expansion coefficients between carbon, epoxy, fiberglass and steel it is quite likely that over the life of the repair, galvanic action will occur due to a break down in the barrier layer. This paper focuses on galvanic action in situations where CFRP is used as an internal reinforcing element in concrete.

2. Previous studies

Four studies were previously conducted to evaluate the electrochemical behavior of CFRP composites (6 mm in diameter, pultruded rods) coupled with active steel (Table 1). In the first study, behavior in chloride-contaminated alkaline solutions was presented [4]. Comparison of potentials and current density measurements

Table 1. Experimental data from previous investigations

Reference	Electrolyte type	Chloride free			Chloride contaminated		
		Potential [1]		Current density [2] (μA cm^{-2})	Potential [1]		Current density [2] (μA cm^{-2})
		mV vs. CSE CFRP	mV vs. CSE Steel		mV vs. CSE CFRP	mV vs. CSE Steel	
4	Saturated calcium hydroxide	−160	−180	10^{-4}–10^{-3}	−210	−620	0.8–1.0
5	Mortar 60% RH	−120	−140	10^{-2}–0.1	−200	−450	0.1–1.2
	Mortar 95% RH	–	–	$< 10^{-4}$	–	–	10^{-2}–0.3
6	Concrete 60% RH	–	–	–	−130	−240	10^{-5}–$2{\cdot}10^{-2}$
	Concrete 80% RH	–	–	–	−190	−300	$2.5{\cdot}10^{-4}$–0.2
	Concrete 95% RH	–	–	–	−200	−370	$2.5{\cdot}10^{-4}$–2.10^{-3}
7	Concrete 85% RH						
	Uncoated Steel	–	–	–	−220	−600	$8{\cdot}10^{-2}$–0.7
	Coated Steel	–	–	–	−200	−530	$2.5{\cdot}10^{-2}$–0.25

(1) Potential just before interconnection.
(2) Current density is the measured current divided by the CFRP surface area.

in these specimens immersed in chloride and chloride-free saturated calcium hydroxide (SCH) solutions showed that chloride contamination could allow galvanic corrosion between CFRP and steel (see Table 1), raising concerns about the degradation of both CFRP and steel [4].

The discovery of galvanic interaction between CFRP and steel in chloride-contaminated SCH solutions, led to additional studies directed towards understanding this phenomenon in mortar [5]. Laboratory experiments were performed to determine the magnitude of galvanic currents that could develop as a result of direct contact between CFRP and steel in mortar under wet-dry cycles [5]. Results obtained showed little galvanic corrosion in steel when coupled with the same CFRP rods in mortar free of chlorides with a 0.5 water to cement (w/c) ratio (Table 1). However, significant galvanic action was observed in chloride contaminated mortar (~3.5% chloride by weight of cement).

The above findings led to a third investigation directed towards identifying environments that were most detrimental. Since CFRP was likely to be used in humid, subtropical aggressive environments, the performance of CFRP and uncoated #3 reinforcing steel bars (rebars) in contact in chloride contaminated concrete was evaluated for different relative humidity (RH) environments ~60, 80, and 95%. The concrete had a water to cementitious ratio of 0.45 and was cast with ~14 kg m^{-3} chloride [6]. Results showed significant galvanic action in the 80% RH chloride contaminated concrete (Table 1). For the other environments the galvanic currents densities were an order of magnitude smaller, indicating that the worst case scenario was obtained when the concrete was exposed to an intermediate humid environment. Nonetheless, the galvanic current densities measured between CFRP and uncoated steel were still small (< 0.2 μA cm^{-2} as in Table 1).

In demonstration bridges constructed using CFRP, epoxy coated steel is usually used as shear reinforcement [8]. In this case, shear reinforcement in the form of vertical steel is tied to the CFRP rods to form a rigid cage that allows the concrete to be placed. During construction, some breaks in the epoxy coating are inevitable especially because the CFRP rod surfaces are rough to enhance bond with concrete. This scenario was modeled in the final study of this series in which the galvanic effect of coated and uncoated steel in chloride-contaminated concrete was compared [7]. In the setup plain (#3) bars and epoxy coated (#4) bars were used. About 0.1% of the surface of the epoxy coated bars was intentionally-damaged to simulate field conditions. Testing was conducted at 85 ± 5% RH (Table 1).

Unlike the previous (third) study, in addition to measurement of potentials and currents during the coupling stage, the corrosion rate of the steel was also monitored before and after the galvanic action between CFRP and steel. The results showed that uncoated steel was unaffected (as in [4]), since the estimated corrosion rates before and after CFRP coupling were similar. In contrast, coupled CFRP and coated steel showed a tenfold increase in the estimated corrosion rate compared to CFRP-uncoated bar couples, suggesting that the worst case scenario for galvanic interaction between CFRP and steel was when the steel rebar is coated but damaged.

All four previous studies focused on galvanic interaction and its effect on steel, but did not include any investigation on how the CFRP rod was affected. This paper presents results of evaluations carried out to identify changes in the electrochemical properties of the CFRP rods due to galvanic action in chloride-contaminated concrete. Electrochemical impedance spectroscopy (EIS) tests were performed before and after galvanic interaction for the entire duration of the study to determine the effect of coupling. Electrochemical parameters were estimated using a software package and changes over time compared. The implications of these findings are discussed.

3. Material properties

3.1. *CFRP*

The 6 mm diameter CFRP rods used in the study were pultruded in the Netherlands using FORTAFIL® 3 (C) continuous carbon fibers produced in the United States that was supplied in the form of a 50 000 filament continuous tow. The carbon fiber diameter was 7 μm and the fiber volume was approximately 53%. The external surface of the rod was covered with a sand grit composite to enhance bond with concrete. The mechanical properties of the composite are summarized in Table 2. Figure 1 shows an optical micrograph of the transverse cross section in the as-received condition. The CFRP rod used in this experiment were tested in the initial, as-received condition.

3.2. *Steel*

Two different reinforcing steel bars (rebars) were used in this investigation: # 3 plain rebar (PR) and # 4 epoxy coated rebar (ECR), 9 and 13 mm in diameter, respectively. Further information regarding PR specimens is presented elsewhere [7]. The carbon content, per mill test report for both PR and ECR specimens was ~0.4 wt%. Since the surface of the ECR could be expected to be damaged during handling and construction, this effect was investigated. The surface of the ECR specimens was mechanically degraded by filing off 0.1% the epoxy paint. The filing marks were typically 0.5 mm wide, 0.2 mm long and ~0.05 mm deep, uniformly spaced and in sufficient numbers to reach the target percentage damage of ~0,1% [3].

Table 2. Carbon fiber and composite properties (from manufacturer specs)

Material properties	Carbon fiber	Composite
Tensile strength	3800 MPa	1450 MPa
Tensile modulus	227 GPa	121 GPa
Ultimate elongation	1.7%	1.5%
Density	1.8 g cm^{-3}	–
Cross section area	4.3×10^{-5} mm^2	29.7 mm^2
Fiber Diameter	7.3 μm	–
Axial thermal expansion	−0.1 $\mu m\ m^{-1}\ ^{\circ}C^{-1}$	25 $\mu m\ m^{-1}\ ^{\circ}C^{-1}$

3.3. *Concrete*

The concrete used for the prisms was made with Type I Portland cement, oolitic limestone as coarse aggregate (with maximum size restricted to 9 mm), silica sand as fine aggregate, and a water-to-cement ratio (w/c) of 0.45. Table 3 lists the concrete mix proportions. A chloride ion contamination of ~14 kg m^{-3} was obtained by adding the stoichiometrically corresponding amount of sodium chloride (NaCl) to the mix water.

4. Experimental procedure

4.1. *Specimen preparation*

A total of twelve 5 × 10 × 20 cm concrete prisms were tested. Four of these were controls and the remaining eight coupled (see Table 4). Uncoated steel was placed in six prisms, and were identified as 'PR' cells. The remaining six prisms were cast with coated steel, and are identified as 'ECR cells' (see Table 4). Each prism had one CFRP rod, one PR or ECR rebar, and one 0.5 cm long centrally placed internal activated titanium (Ti/TiO_2) reference electrode (IRE). Figure 2 shows the cell configuration.

The end of the CFRP rod was placed outside the concrete prism to avoid direct contact of the fiber tips to the electrolyte (e.g. concrete) to ensure that only the transverse electrochemical behavior of the composite was investigated. An epoxy plug was placed at both ends of the ECR specimens to avoid corrosion at the exit points of the protruding steel.

The nominal surface area of both the CFRP and PR rods in contact with the concrete was ~32 cm^2 while only ~0.1 cm^2 of the steel area in the ECR bar that had

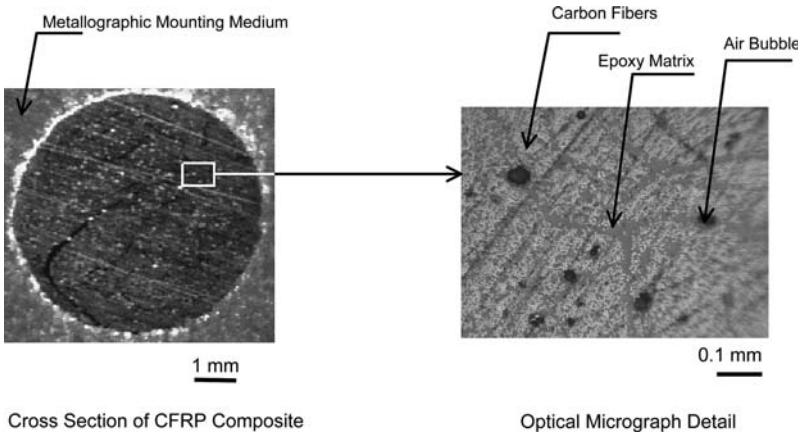

Fig. 1. Cross section micrograph of the CFRP.

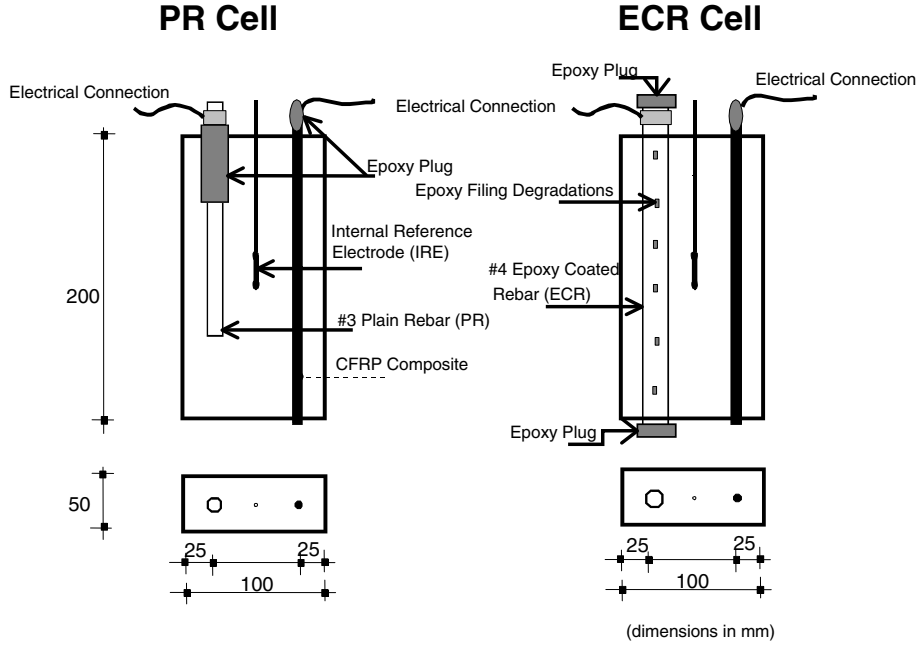

Fig. 2. Cell configurations.

been removed by filing was similarly in contact. The filings were made to simulate damage that could be expected to occur during construction.

Individual electrical connections of both, steel and CFRP rod, were made to external wiring. In particular, a CFRP contact resistance of $<1\ \Omega$ was achieved with 9 mm long stainless steel screws placed inside a drilled-and-tapped hole in one of the CFRP ends. A copper cable was attached to the screw. After placing 5 mm of the screw inside the CFRP, a carbon conductive paint film was applied to the connection, to ensure electrical continuity of the entire CFRP rod. An epoxy coating encased the connection to avoid possible moisture-induced external galvanic effects between the screw and the CFRP rod. Further details of this type of connection are presented elsewhere [6].

The experiments (all at $22 \pm 2^{\circ}C$ and $\sim$80% R.H.) involved ten consecutive stages: (a) Curing stage (from day 0 to day 21), (b) Stabilization stage (from day 22 to day 61), (c) Four coupling stages (c1 through c4), (d) Three uncoupling stages (u1 through u3, in between each coupling stage), and (e) A final uncoupling stage (u4), in which the galvanic couples were permanently disconnected for future investigation. The four coupling-uncoupling stages lasted 283 days (beginning at day 62 and ended day 345). Detailed explanation of each one of these stages is presented elsewhere [7]. The length of the curing and stabilization stages was chosen such that the potential of steel and CFRP was stable before coupling of the two materials.

Table 3. Mix proportions for concrete prisms

Material	Contents (kg m^{-3})
Type I portland cement	391
Water	177
Fine aggregate (silca sand)	776
Coarse aggregate (limestone, 1 cm max. nominal size)	866
Calculated total Cl^- concentration	14

Table 4. Specimen description

Steel type	Control	Coupled
Uncoated	PR3, PR4	PR1, PR2, PR5, PR6
Coated	ECR3, ECR4	ECR1, ECR2, ECR5, ECR6

4.2. *Potential and galvanic current measurements*

Potential measurements of the CFRP and steel were made regularly using a 200 MΩ internal impedance DC voltmeter. These measurements were made with respect to the titanium IRE that was periodically calibrated against an external copper/ copper-sulfate electrode (CSE). During the coupling stages (c1–c4), the potentials of the CFRP and steel specimens were measured in the "instant-off" condition to avoid errors due to ohmic potential drop in the electrolyte (concrete). A CMS100 corrosion measurement system from Gamry Instruments, Inc., configured as a zero resistance ammeter (ZRA) was used to measure the galvanic currents between the CFRP and steel specimens during the coupling stages (c1 through c4).

4.3. *EIS*

To determine if the CFRP was adversely affected by galvanic interaction, EIS measurements were performed on the CFRP rod during the entire experimental period.

EIS testing was performed using a three-electrode configuration under potentiostatic control using a EG & G Princeton Applied Research 273 potentiostat under computer control. The CFRP rod served as the working electrode and an external sponge-padded, titanium mesh served as the counter electrode. The frequency range was varied from 1 to 100 kHz using a +10 mV rms sine wave superimposed on the CFRP open circuit potential. Impedance scans were collected at various times of exposure (stages a, b, and the four uncoupling stages, u1 through u4). Each impedance spectrum, Z, was displayed as a Nyquist plot (Real part of Z vs. Imaginary part of Z) at low and high frequencies, and Bode Magnitude or Bode Phase plots (log |Z| vs. Log frequency, and phase angle vs. log frequency, respectively). Visual inspection of the Nyquist graphs (not shown in this publication) was employed to predict the CFRP equivalent circuit which best matched the test data. The parameter values of the equivalent circuit proposed were determined using the nonlinear least square fit (NLLSF) analysis of the Equivalent Circuit software from the University of Twente [9].

4.4. *Microscope analysis*

A microscope analysis of the CFRP cross sections before and after galvanic interconnection was additionally performed. Since the test specimens are still under analysis, the specimens examined were taken from a previous investigation in which they were identically tested but in SCH solution [4]. Scanning Electron Microscope (SEM) photographs were taken to determine if the galvanic interaction between both materials in SCH solutions, with and without chlorides, changed the microstructure of the CFRP composite.

After a 90-day exposure period, four CFRP rods were taken out of the SCH solution and allowed to dry for 7 days in a laboratory environment ($20 \pm 2\ ^{\circ}C$, $65 \pm 5\%$ RH). Two of these specimens were taken from the chloride-free SCH solution and the other two from the chloride-contaminated SCH solution. Test specimens were then cut into three sections of the same length using a hand saw. These were then mounted in a two-component epoxy for handling it easily. Two were placed transversely and the third lengthwise to allow examination in both the transverse and longitudinal directions. A 240 grit silicon carbide paper was used under running distilled water to clean the surface further. This abrasion also removed a thin insulating layer of resin-rich material to expose clean fiber surfaces. Following this operation, care was taken not to contaminate the composite surface with hand oils.

The four specimens were then photographed using a SEM. The cross-section was photographed as six to eight segments. The micrographs of the segments were then glued together to obtain a full cross section view of the CFRP rod.

5. Results and discussion

5.1. *Galvanic potentials*

Before coupling, the steel average potentials were significantly more negative than the CFRP potentials. CFRP potentials before galvanic coupling with steel were typically -200 ± 100 mV vs. CSE. The potential values of PR and ECR specimens in all twelve cells were characteristic of actively corroding steel [3], as expected due to the high chloride ion content of the concrete. Steel potentials were quite negative (-600 ± 100 mV CSE in average) during the curing and the stabilization stages. After coupling the system reached a mixed potential dominated by that of the steel which was always the anode. In the later uncoupled periods steel potentials fluctuated but were still typically 200–500 mV more negative than the CFRP. More details of the measured values may be found in [6].

5.2. *Galvanic currents*

The galvanic currents measured during the four coupling stages (c1 through c4) spanned between 0.06 and 15 μA regardless of the steel type (PR or ECR). The reason for this is not evident at this time. The galvanic currents measured during the four coupling stages indicated that the anodic current densities applied to the steel were as high as 2 and 100 $\mu A\ cm^{-2}$ for PR and ECR cells, respectively [7]. These high levels of additional anodic current density by themselves could seriously reduce service life of a concrete structure to as little as a few years [10–11].

5.3. *Potential vs. current of the coupled specimens*

Figure 3 shows a composite plot of the overall "instant-off" potential vs. log galvanic current density (measured galvanic current divided by the CFRP surface area: 32 cm^2) over the four coupling periods for both cell types. The data in Figure 3 delineate behavior typically observed in polarization tests of CFRP in concrete [6].

The data corresponding to the PR and ECR cells tended to separate into two distinct populations. For PR cells, the potentials were quite stable (between −550 and −650 mV vs. CSE, with average −607 mV), and the galvanic currents densities fluctuated between 0.004 and 0.3 $\mu A\ cm^{-2}$ (average 0.048 $\mu A\ cm^{-2}$). In contrast, ECR showed low levels of polarization (potential greater than −500 mV), which the behavior of this cells approximated that of a system under activation polarization with Tafel slope on the order of 100–200 mV/decade, typical of oxygen reduction [12]. At stronger polarization (potential less than −500 mV), the ECR cells showed indications of diffusional limitation of the oxygen supply as observed from the changed in slope of the current-potential data (see Figure 3) [12].

Most of the galvanic potentials for CFRP-PR couples were between −550 and −700 mV vs. CSE, as compared

to the wider potential range for the CFRP-ECR couples: between −300 and −600 mV vs. CSE. It appears that the CFRP-PR couples gave higher polarization than the CFRP-ECR ones. In addition, the galvanic current densities observed for CFRP-PR couples were one order of magnitude smaller than the CFRP-ECR couples. These results suggest that, even though higher polarizations were reached between CFRP-PR couples, the galvanic current densities of the CFRP-PR were more benign than CFRP-ECR couples since the CFRP-PR current densities were smaller than the CFRP-ECR ones for similar galvanic potential. This indicates that the galvanic interaction between the two materials (CFRP and steel) in concrete is increased when the steel is coated.

5.4. *EIS tests*

Figures 4a, b and 5a, b show typical Bode magnitude and Bode phase plots for one control (ECR4) and one coupled (ECR1) CFRP rod, respectively. The EIS spectra for the uncoupled CFRP rods remained more or less the same during the entire experiment, as may be observed from Figure 4. For coupled specimens (Figure 5), three basic changes with time of coupling are noticed: (1) the impedance value decreases, (2) the slope of the impedance magnitude decreases, and (3) the Bode phase plot is depressed. A possible explanation for these changes is that the electrochemically active surface area is increasing [13–14].

To deduce possible interfacial changes on the composite, EIS analysis, using equivalent circuit theory was applied. The Randles equivalent circuit was used in this investigation to fit the experimental impedance. It consisted of three electrochemical parameters: solution and CFRP polarization resistance (R_S and R_P, respectively), and a constant phase element (CPE) related to the surface state of the rod (porous electrodes) [13–14].

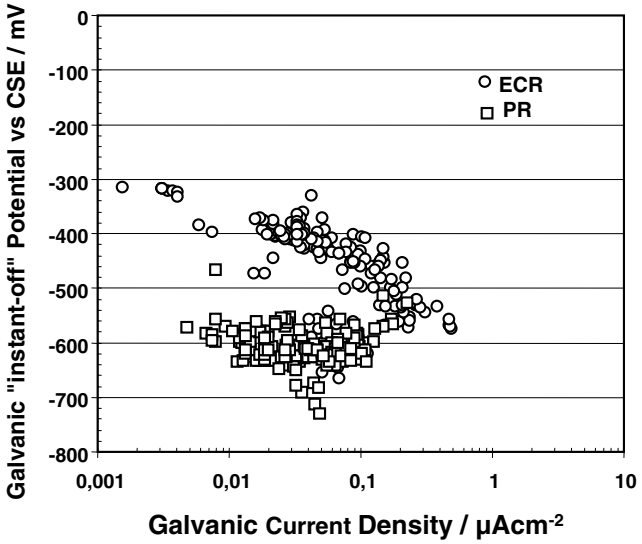

Fig. 3. Potential vs. Current density composite plot.

The impedance of a ideal capacitor is $Z = -1/jwC$, where j is $(-1)^{1/2}$, w is the frequency, C is the capacitance. For a CPE is $Z = 1/(jw)^n Y_0$. Thus, the CPE can be thought of as a non-idealized capacitor that has magnitude equal to "Y_0," and an adjustable exponent "n". These parameters were estimated as a function of time using the University of Twente's software package [9].

Figures 6 and 7 presents the CPE parameter estimates ("Y_0" and "n"), as a function of time for both PR and ECR cells. The increase of "Y_0" and decrease of "n" with time supports the idea of the active surface area increase. Figure 8 shows the changes of Y_0 relative to the curing stage estimate. The values plotted in Figure 8 were obtained using Equation (1):

$$\Delta Y_0 = \frac{Y_{0-\text{stage}} - Y_{0-\text{ini}}}{Y_{0-\text{ini}}} \tag{1}$$

where $Y_{0\text{ - }ini}$ and $Y_{0\text{ -}stage}$ are the estimated values of Y_0 at the beginning of the curing stage, and at the end of the other stage periods, respectively. All ΔY_0 estimates for the control, PR and ECR cells, were obtained as an average of four specimens. As seen from Figure 8, the average ΔY_0 estimates for the control cells had small fluctuations. On the other hand, the average ΔY_0 estimates for PR cells increased up to 50% due to the

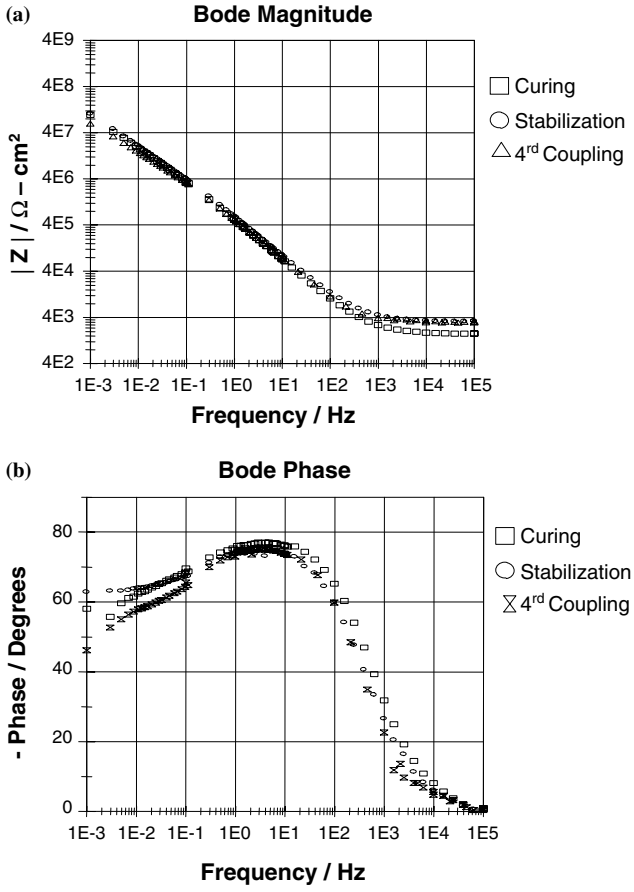

Fig. 4. (a) Typical bode magnitude diagram for a control CFRP strand; (b) Typical bode phase diagram for a control CFRP strand.

galvanic interaction between the two materials (CFRP and steel). In contrast, the ΔY_0 estimates for ECR cells were nearly double (180%) the value of the initial estimate obtained during the curing stage. The results showed that the CFRP interface was affected due to the galvanic effect of active steel, and this effect was aggravated when connected with mechanically degraded coated steel rebar.

Figure 9 quantifies the total cathodic action of each couple (CFRP-PR and CFRP-ECR) by plotting the total electrical charge passed through the composite (in mA-hr) and the ΔY_0 estimates. As observed from the trend lines, there is an instantaneous increase of the ΔY_0 estimates when CFRP is connected with coated steel, as compared to the gradual increase of ΔY_0 for the uncoated steel, but still the values are quite similar.

The increased electrode area could result from either moisture penetration into the composite, or roughening of the exposed composite surface (fiber/matrix interface breakdown), or caused by composite/concrete interface changes [13–14]. Since no significant change in the electrochemical parameters, Y_0 and n, was observed in the control specimens (see Figures 6 and 7), moisture penetration could not have been a factor. It is apparent that the application of cathodic polarization has a major

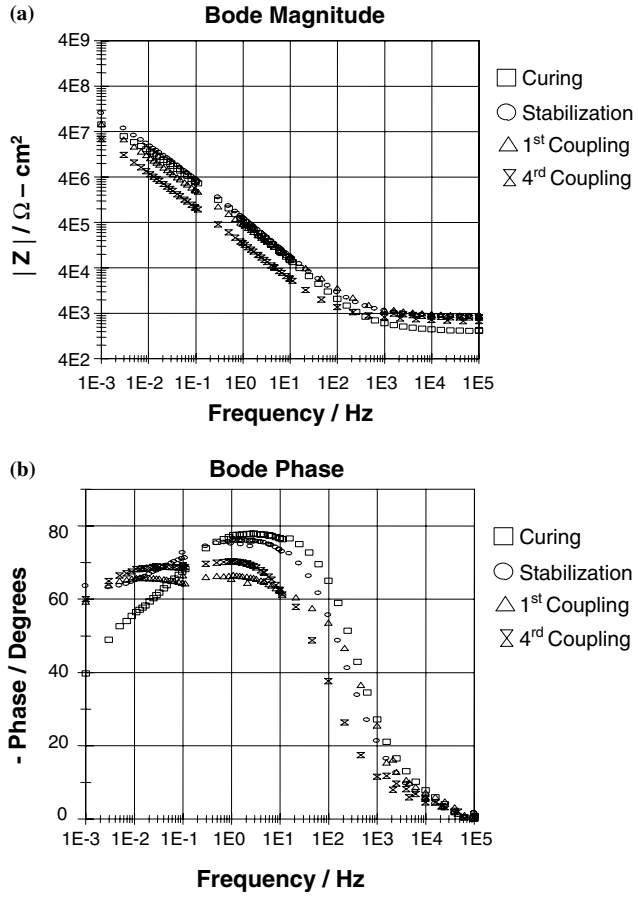

Fig. 5. (a) Typical bode magnitude diagram for a coupled CFRP strand; (b) Typical bode phase diagram for a coupled CFRP strand.

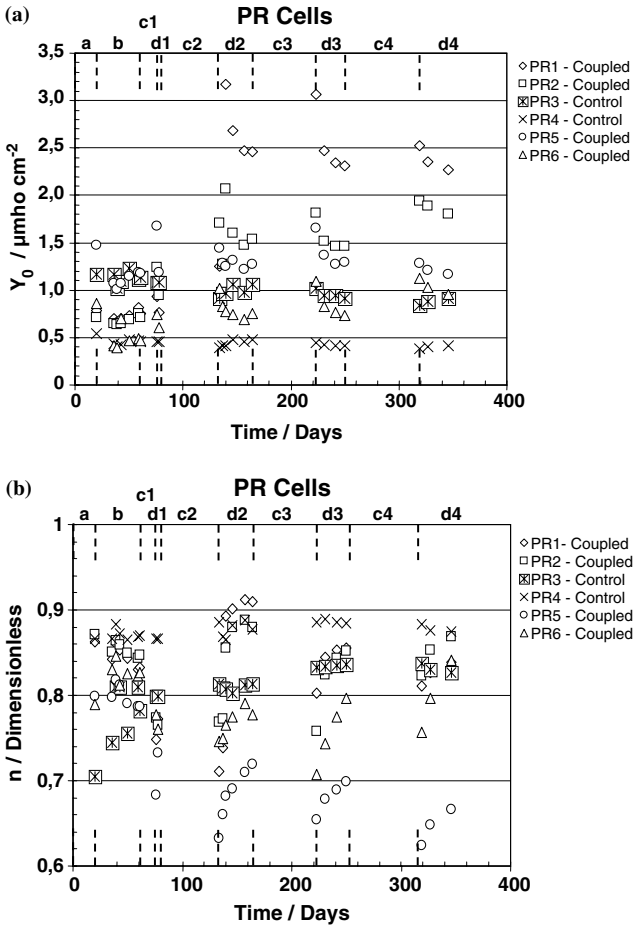

Fig. 6. (a) Estimated values of Y_0 vs. Time of PR cells; (b) Estimated values of n vs. Time of PR cells.

effect on the electrochemical properties of this composite rather than only moisture penetration.

The impedance data suggests that the composite surface is changing in a way so as to have porous electrode characteristics [14]. A tilting of the Bode Magnitude curve (see Figure 5) and a shift to lower frequencies both signal an increase in electrode roughness, and thus an increase of the capacitive behavior of the composite (increase in Y_0). Given the insulating nature of the epoxy matrix, the changes in the Bode curves suggests that an increasing amount of carbon fiber is being exposed to the electrolyte (i.e. concrete). This increase in exposed fiber area means that the fiber/matrix interface is being lost, which can result in strength losses over time. To evaluate these changes on the composite, microscopy analysis was performed and the results were as follows.

5.5. *Microscopy analysis*

As mentioned earlier, a microscopy study was performed on four of the CFRP rods from a previous investigation in which they were immersed in SCH solutions [4]. The cathodically polarized CFRP rod displayed a well defined porous composite surface at the perimeter much greater than the initial sand grit placed

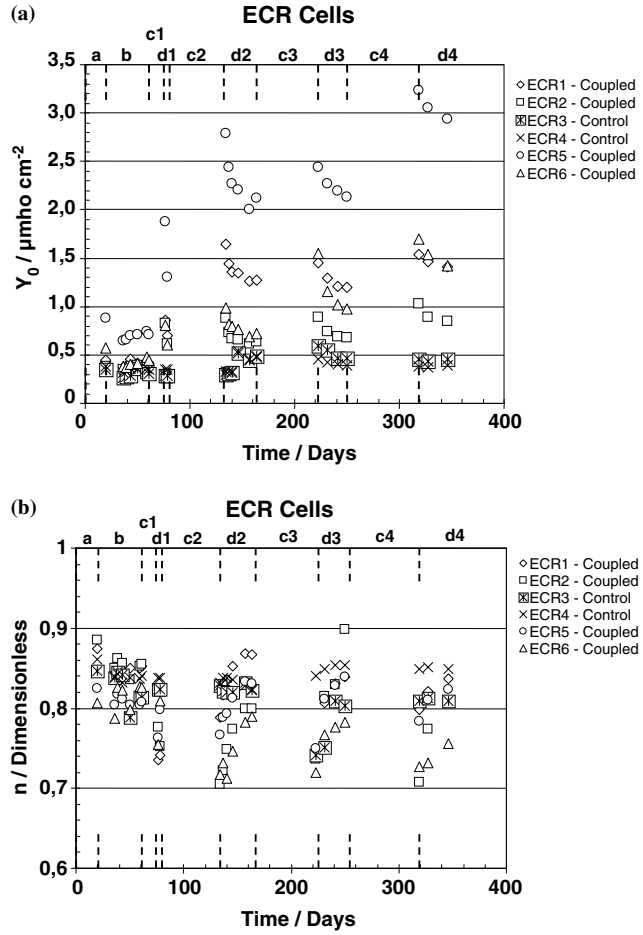

Fig. 7. (a). Estimated values of Y_0 vs. Time of ECR cells (b). Estimated values of n vs. Time of PR cells.

on the original composite surface to increase its anchorage with concrete. Based on EDX analysis performed on this specimen, the additional material that formed on the composite surface consisted of calcium hydroxide nodules, indicating that the galvanic interaction apparently attracts calcium ions to the surface of the composite. This may transform the external interface of the composite and thus the EIS changes observed might be due to the formation of this new interface CFRP/calcium nodule.

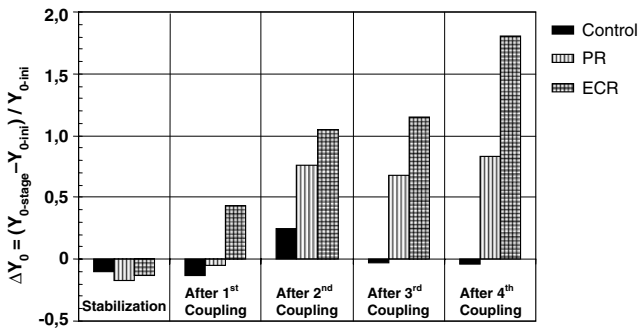

Fig. 8. Y_0 Variation estimates from initial calculations at curing.

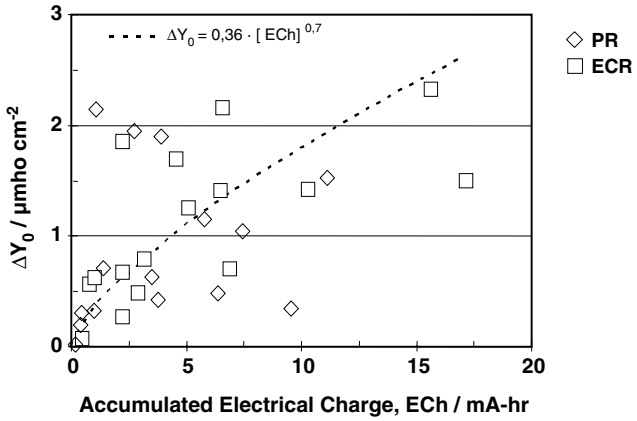

Fig. 9. Change in Y_0 from total cathodic action by the electrical charge (ECh).

On the other hand, the void difference between non-polarized and polarized specimens in this microscopy analysis was inconclusive. Additional voids due to possible matrix degradation were not detected in the cross sections of specimens affected by galvanic interaction with active steel, indicative of a possible fiber/matrix breakdown. Thus, it appears that EIS changes were primarily due to new interface formation at the cross section. Since deposition of calcium can adversely affect the CFRP rod's bond with concrete, galvanic coupling of CFRP with active steel in chloride-contaminated concrete may lead to poorer structural performance.

The results indicate that EIS is potentially a very useful tool for the characterization of CFRP composite interfacial stability. The impact of the results presented here in combination with mechanical properties changes due to galvanic interaction is currently being examined and results will be presented in the future.

6. Conclusions

Laboratory tests were conducted to investigate if galvanic action between a CFRP rod and coated or uncoated steel, arising from direct contact between the two materials (in chloride-contaminated concrete), produced changes in the electrochemical behavior of the CFRP composite.

Galvanic coupling between CFRP and coated or uncoated steel in this media produced anodic currents on the steel. The steel dominated the potential of the galvanic couple. The galvanic current density measured between CFRP and uncoated steel was quite small (average 0.048 μA cm^{-2}). On the other hand, when the CFRP composite was interconnected with mechanically degraded coated steel rebar (with a CFRP:steel area ratio of 10:1), the nominal steel current densities were as large as 100 μA cm^{-2}.

EIS tests were performed to non-destructively estimate the changes in the electrochemical parameters of CFRP due to galvanic interaction with active steel. EIS results have shown that cathodic polarization of CFRP

composites may produce an increase in electrode roughness and possible debonding between the composite and the surrounding concrete. These observations were aggravated when CFRP was coupled with epoxy coated steel.

Optical microscopy provided visible evidence of interface changes of the composite surface. The cross section of a specimen affected by galvanic interaction with active steel displayed a well defined porous composite surface at the perimeter that extended beyond the initial sand grit placed on the original composite surface to enhance bonding with the concrete. Since such interface change affects bonding, it is reasonable to conclude that galvanic coupling of CFRP with active steel in chloride-contaminated concrete may lead to poorer structural performance. This adverse effect needs to be carefully validated in the future.

Acknowledgements

The author is indebted to the University of South Florida and the Mexican Council of Science and Technology (CONACYT), for partial support of this investigation under the Inter-American Materials Collaboration, CIAM 2002, project No. U42362-K. The author also acknowledges funding from the Instituto Mexicano del Transporte (Mexican Transportation Research Institute) Queretaro, Mexico, for the preparation of this manuscript.

References

1. ACI 440R-96, 'State-of-the-Art Report on Fiber Reinforced Plastic Reinforcement for Concrete Structures'. American Concrete Institute, Farmington Hills, MI.
2. L.C. Hollaway and J. Cadei, *Progr. Struct. Eng. Mater.* **4** (2002) 131.
3. A.A. Sagüés, 'Corrosion of Epoxy Coated Rebar in Florida Bridges,' Final Report to Florida D.O.T., WPI No. 0510603, Available from FDOT Research Center, Tallahassee, FL.
4. A.A. Torres-Acosta, 'Electrochemical Behavior of Carbon Fiber-Reinforced Plastic (CFRP) Strands in Alkaline Solutions,' Proceedings XVIII Congress of the Mexican Society of Electrochemistry, Chihuahua, Chihuahua, Mexico, May 26–30, 2003.
5. A.A. Torres-Acosta, *J. Compos. Construct.* **6** (2002) 112.
6. A.A. Torres-Acosta, A.A. Sagüés, and R. Sen, Paper No. 98648, 1998 NACE Conference (NACE International, Houston, TX, 1998).
7. A.A. Torres-Acosta, *J. Compos. Construct.* **6** (2002) 116.
8. S. Rizkalla and G. Tadros, *Concrete Int.* **16** (1994) 42.
9. B.A. Boukamp, 'Equivalent Circuit (EQUIVCRT.PAS) Users Manual', University of Twente, Netherlands, Report CT89/214/128, 1989.
10. A.A. Torres-Acosta and A.A. Sagüés, 'Concrete Cover Cracking due to Corrosion of the Reinforcing Steel', Proceedings of 5th CANMET/ACI International Conference on Durability of Concrete, (editor V. Malhotra), American Concrete Institute, SP-192, Farmington, Hills, Michigan, USA (2000) pp. 591–611.
11. A.A. Torres-Acosta and M. Martínez-Madrid, *J. Mater. Civil Eng.* **15** (2003) 344.
12. A.A. Sagüés, M.A. Pech-Canul and A.K.M. Shahid Al-Mansur, *Corrosion Sci.* **45** (2003) 7.
13. S.R. Taylor, *Compos. Interfaces* **2** (1994) 403.
14. S.R. Taylor, F.D. Wall and G.L. Cahen, *J. Electrochem. Soc.* **143** (1996) 449.